ELSEVIER

Journal of Hydrology 256 (2002) 120–141

Journal of Hydrology

www.elsevier.com/locate/jhydrol

Multivariate stochastic downscaling model for generating daily precipitation series based on atmospheric circulation

Jiří Stehlík[a,*], András Bárdossy[b,1]

[a]*Department of Physical Geography and Geoecology, Charles University in Prague, Faculty of Science, Albertov 6, Prague 2, 12843 Czech Republic*

[b]*Institute of Hydraulic Engineering, University of Stuttgart, Pfaffenwaldring 61, 70550 Stuttgart, Germany*

Received 20 October 2000; revised 14 September 2001; accepted 24 September 2001

Abstract

The goal of the paper is to present a model for generating daily precipitation time series and its applications to two climatologically different areas. The rainfall is modeled as stochastic process coupled to atmospheric circulation. Rainfall is linked to the circulation patterns using conditional model parameters. Any kind of circulation pattern classification can be used for this purpose. In this study a new fuzzy rule based method of circulation patterns classification was used. The advantage of this classification technique is the fact that in contrast to common circulation patterns classifications its objective is to explain the variability of local precipitation. It means that the circulation patterns explain the relation between large-scale atmospheric circulation and surface climate (precipitation). Therefore the circulation patterns obtained by this classification method are suitable as input for the subsequent precipitation downscaling. The model was successfully applied in two regions with different climate conditions: Central Europe (Germany) and Eastern Mediterranean (Greece). Several tests like comparison of mean seasonal cycles, comparison of mean values and deviations of yearly totals and other standard diagnostics showed that simulated values agree fairly well with historical data.

Keywords: Precipitation; Downscaling; Circulation patterns; Stochastic modeling

1. Introduction

The purpose of this paper is to present a stochastic model for generating daily precipitation series and its applications in two regions with different climate conditions, namely Central Europe (Germany) and Eastern Mediterranean (Greece).

It is not possible to generate long term precipitation series by means of deterministic methods. This fact was proved by many studies dealing with chaotic behavior of rainfall data (e.g. Rodriguez-Iturbe et al., 1989; Sharifi et al., 1990; Jayawardena and Lai, 1994; Sivakumar et al., 1998; Sivakumar, 2000). The highly nonlinear relationships among variables governing the climate system cause the effect known as sensitive dependence on initial conditions as investigated for the first time by Lorenz (1969). However, for longer time scales a correlation was found e.g. between North Atlantic sea surface temperature anomalies and rainfall data by using monthly gridded averages of land based raingauge observations (Colman and Davey, 1999).

* Corresponding author. Tel.: +420-2-4403-2327; fax: +420-2-4403-2357.

E-mail addresses: stehlik@chmi.cz (J. Stehlík), bardossy@iws.uni-stuttgart.de (A. Bárdossy).

[1] Tel.: +49-711-685-4663; fax: +49-711-685-4746.

0022-1694/02/$ - see front matter
PII: S0022-1694(01)00529-7

The major problem of mathematical modeling of daily precipitation series is their spatial and temporal variability and clustering effects both in time and space. These effects have natural causes like the movement of atmospheric fronts. Dealing with simulation of precipitation time series is important not only from the pure scientific point of view but it has also a lot of practical consequences in hydrology. The generated series can be used for making predictions of recurrence intervals of various extremes like dry periods or extreme precipitation events. Using generated extreme precipitation events as input in hydrological models enables to asses their hydrological influence. One important need of artificial generating of precipitation series insists in the fact that the observed series are very often too short or not enough spatially resoluted for the purposes of hydrological modeling. The precipitation generators make it possible to derive parameters from the observed series and then to generate long series with high spatial resolution. Stochastic rainfall simulators can also provide an input for hydrological models in order to estimate the peak discharges for design purposes on catchment with only limited available data. For example a stochastic rainfall simulator which differentiates between high and low intensity events was developed to drive a version of TOPMODEL (Blažková and Beven, 1997).

The first attempts for precipitation modeling were done by means of simple autoregressive moving average (ARMA) models for annual precipitation totals. Also the monthly totals can be modeled with the help of appropriate transformations. In case of daily rainfall the problem of time intermittence occurs which cannot be solved by a classical time series models because these assume continuous and mostly normal distribution of variables. However, the daily precipitation series are discrete–continuous: discrete to describe dry spells and continuous for modeling of precipitation amounts on wet days. The same problem occurs in space too. As rainfall does not always cover the whole area, spatial intermittence also has to be considered.

Markov models and Markov renewal models are often applied for modeling of precipitation occurrence and duration (Berger and Goossens, 1983; Foufoula-Georgiou and Lettenmaier, 1987). Chang et al. (1984) used a discrete ARMA model for modeling of sequences of dry and wet days. Wilks (1989) developed a model for precipitation occurrence and amounts with parameters depending on monthly totals. Review of models for continuous modeling of precipitation was done by Rodriguez-Iturbe et al. (1987). Stochastic space-time model for simultaneous modeling of precipitation on several locations was developed by Binark (1979). The model of Hay et al. (1991) simulates precipitation depending on regional weather conditions. Wilson et al. (1991, 1992) introduced precipitation model which takes large-scale atmospheric circulation into account. The links between circulation and weather can also be expressed in terms of multiple regressions between either grid point values or intensities of circulation variability modes (principal components) and precipitation (Huth, 1997). Katz and Parlange (1993, 1996) performed the stochastic modeling of time series of daily precipitation amount conditional on a monthly index of large-scale atmospheric circulation patterns (CPs). Koutsoyiannis and Xanthopoulos (1990) introduced model which generates rainfall from monthly to hourly scales. Bárdossy and Plate (1992) developed a multidimensional stochastic model for space-time distribution of daily precipitation. The rainfall is linked to atmospheric circulation patterns using conditional distributions and conditional spatial covariance functions. The model is a transformed conditional multivariate autoregressive model with parameters depending on the atmospheric circulation pattern. The model was applied in the catchment of the river Ruhr using the classification scheme of the German Weather Service.

There is a good reason for relating rainfall characteristics to large-scale atmospheric circulation. Several studies proved relationships between circulation patterns and climatic variables. Bürger (1958) studied the relationship between the atmospheric circulation patterns and mean, maximum and minimum daily temperatures, precipitation amounts and cloudiness using the time series from 1890 to 1950 measured at four German cities (Berlin, Bremen, Karlsruhe and Munich). He found a good correspondence between climatic variables and atmospheric circulation. Lamb (1972, 1977) stated that even the highly varying precipitation is strongly linked to the atmospheric circulation. Trenberth (1990) analyzed the importance of atmospheric dynamics in climate

change. He also states that atmospheric circulation is the major link between regional changes in climate variables.

Another problem is downscaling of precipitation under climate change conditions. Global circulation models (GCM) do not provide realistic precipitation series even for the present climate scenarios. Even if it would be the case it would not be possible to generate precipitation time series for smaller regions or selected locations because of coarse space resolutions of GCM (IPCC, 1996). However, it is possible to downscale precipitation behavior from the GCM air pressure or geopotential height outputs. A lot of attention has been paid in the last years to the problem of statistical downscaling from GCM (e.g. Karl et al., 1990; Wigley et al., 1990; Hay et al., 1992; von Storch et al., 1993; Wilby et al., 1998a; Wilby et al., 1999; Huth and Kyselý, 2000). A review of methods for GCM precipitation downscaling was done by Giorgi and Mearns (1991) and Wilby and Wigley (1997). Wilby et al. (1998b) proposed a procedure for comparing the performance of various precipitation downscaling models. The overview of techniques for assessing the effects of climate change on water resources has been done by Leavesley (1994).

A method for classifying circulation patterns based on precipitation observations was presented in Bárdossy et al. (2001). The precipitation characteristics of CPs from most CP classification methods are studied 'ex post'. The mean precipitation behavior conditioned on the CPs is usually determined after the classification. The advantage of the classification method of Bárdossy et al. (2001) is that the objective is to define CPs so that they explain the variability of precipitation in a locally specific functional form. Therefore the CPs explains the dependence between the large-scale atmospheric circulation and the surface climate (precipitation). Therefore the circulation patterns obtained by this classification method are very suitable as input for the subsequent precipitation downscaling. The circulation patterns are defined using geopotential pressure heights in a regular grid over Europe and eastern Atlantic. The model uses fuzzy logic concept for circulation patterns definitions. The fuzzy rules are obtained automatically using an optimization of the performance of the classification. The performance of a classification is measured by its conditional rainfall frequencies and rainfall amounts. The methodology was applied in Central Europe (Germany) and Eastern Mediterranean (Greece). The circulation pattern classifications from the study mentioned earlier are used in this paper as one of the inputs for generating precipitation time series.

The paper is organized as follows. In Section 2 the models both for circulation patterns classification and downscaling of precipitation will be described. In Section 3 case studies for Germany and Greece will be given. Section 4 consists of a discussion and conclusions.

2. Methodology

The generated rainfall series take the daily circulation patterns into consideration using conditional probabilities. In this study, a new automated fuzzy rule based classification of circulation patterns was applied (Bárdossy et al., 2001). As mentioned earlier, this classification technique was developed with the aim to serve as a basis for subsequent precipitation downscaling because the task of the method is to explain the variability of precipitation in a given area.

2.1. Circulation patterns classification

Usually circulation patterns classification is done on statistical basis or meteorological considerations. For the regions of both case studies subjective classifications exist — CP classification of Baur et al. (1944) and Hess and Brezowsky (1969) for Central Europe and Maheras (1988, 1989) for the East Mediterranean territory. This scheme was used by Mamassis and Koutsoyiannis (1993, 1996) for the analysis of intense rainfall and flood events in Greece, including stochastic modeling. In the presented study, an automated CP classification was performed with the task to achieve an optimal precipitation downscaling.

The daily circulation patterns were defined using 500 and 700 hPa geopotential pressure heights and precipitation amounts from several climate stations. The classification based on fuzzy rules was applied. The advantage of this classification is that it is objective, automated and takes precipitation behavior in a certain region into account. The task of the classification is to obtain circulation patterns, which differ as much as possible from the average precipitation

behavior, it means that the objective is to get some wet and some dry circulation patterns in frame of one classification. The position of the highs and lows is given in the form of fuzzy rules. They provide a framework for dealing with vague and/or linguistic information in modeling. Fuzzy logic accepts overlapping boundaries of sets: instead of elements belonging or not belonging to a given set, partial membership in any set is possible.

Here the classification approach uses fuzzy sets, which may be considered as a mathematical representation of imprecise statements as 'high pressure' or 'above normal'. Each circulation pattern is described by a set of fuzzy rules. Then the classification is done by selecting the pattern for which the fulfillment grade of the corresponding rules is the highest. For more details refer to Bárdossy et al. (2001).

2.2. Precipitation downscaling model

2.2.1. Mathematical basis

Both spatial and temporal intermittence causes problems in the mathematical modeling of precipitation on the daily basis. Usually the probability of occurrence of dry days is relatively high and the rainfall amounts on days with precipitation are described by means of continuous distribution. Therefore random variables with mixed distributions are required to describe daily precipitation. Another problem occurs in the clustering of wet and dry day occurrence. This clustering has natural causes and was usually modeled with the help of appropriate distributions, for example obtained using Neymann-Scott models (Rodriguez-Iturbe et al., 1987). In the time-space model clustering is the consequence of the persistence of atmospheric circulation patterns.

The space time model is a modified version of the model described in Bárdossy and Plate (1992). Let $\mathbf{A} = \{\alpha_1, \ldots, \alpha_n\}$ be a set of possible atmospheric circulation patterns. Let $\tilde{A}_t$ be the random variable describing the actual atmospheric circulation, taking its values from $\mathbf{A}$. Let the daily precipitation amount at time t and point u in the region U be modeled as the random function $Z(t,u)$, u in U. The distribution of rainfall amounts at a selected location is skewed. In order to relate it to a simple normally distributed random function $W(t,u)$ (for any locations $u_1, \ldots, u_n$ the vector $(W(t,u_1), \ldots, W(t,u_n))$ is a multivariate normal random vector) the following power transformation relationship is introduced:

$$Z(t,u) = \begin{cases} 0 & \text{if } W(t,u) \le 0 \\ W^{\beta}(t,u) & \text{if } W(t,u) > 0 \end{cases} \quad (1)$$

Here β is an appropriate positive exponent. This way the mixed (discrete–continuous) distribution of $Z(t,u)$ is related to a normal distribution. As the process $Z(t,u)$ depends on the atmospheric circulation pattern, the same applies to $W(t,u)$. The reason for this transformation is that multivariate processes can be modeled much easier if the process is normal. Further the problem of intermittence can also be handled this way, as the negative values of W are declared as dry days and dry locations. The exponent β is needed as the distribution of precipitation amounts is usually much more skewed than the truncated normal distribution.

The relationship between $W(t,u)$ and the circulation pattern $\tilde{A}_t$ is obtained through the rainfall process $Z(t,u)$ using Eq. (1).

For the subsequent development let us introduce the following notation:

$$\mathbf{W}(t) = (W(t,u_1), \ldots, W(t,u_n)) \quad (2)$$

$$\mathbf{Z}(t) = (Z(t,u_1), \ldots, Z(t,u_n)) \quad (3)$$

The expectation of $W(t,u)$ for a given CP is:

$$w_i(t^*,u) = E[W(t^*,u)|\tilde{A}_t = \alpha_i] \quad (4)$$

where t^* stands for Julian date. It means, that the annual cycle of expectations is taken into account. To simplify the following development the vector of the expectations of $W(t,u)$ is introduced:

$$\mathbf{w}_i(t^*) = (w_i(t^*,u_1), \ldots, w_i(t^*,u_n)) \quad (5)$$

The random process describing $\mathbf{W}(t)$ is described by using the following equation:

$$\mathbf{W}(t) = r(t^*)(\mathbf{W}(t-1) - \mathbf{w}_{i'}(t^*-1)) + \mathbf{C}_i(t^*)\mathbf{\Psi}(t) + \mathbf{w}_i(t^*) \quad (6)$$

where

$$\mathbf{\Psi}(t) = (\psi(t,u_1), \ldots, \psi(t,u_n)) \quad (7)$$

Fig. 1. Location of German precipitation stations used for CPs optimization and subsequent downscaling.

is a random vector of independent $N(0,1)$ random variables. Again the symbol t is valid for the day of the simulation, whereas t^* holds for the Julian date corresponding to the actual day t. The symbol i stands for the circulation pattern on day t^* and the symbol i' for the previous day $t^* - 1$. $r(t^*)$ is autocorrelation of one day time lag. Lag 1 autocorrelations of the daily precipitations do not vary strongly in space — the model assumes them to be equal, due to the large-scale features causing precipitation. This assumption might not hold for shorter time steps. The autocorrelation is independent of the circulation pattern but dependent on an annual cycle, which is approximated by using the Fourier series:

$$r(t^*) = \frac{A_0}{2} + \sum_{k=1}^{K} (A_k \cos(k\omega t^*) + B_k \sin(k\omega t^*)) \quad (8)$$

Fig. 2. Location of Greek precipitation stations used for CPs optimization and subsequent downscaling.

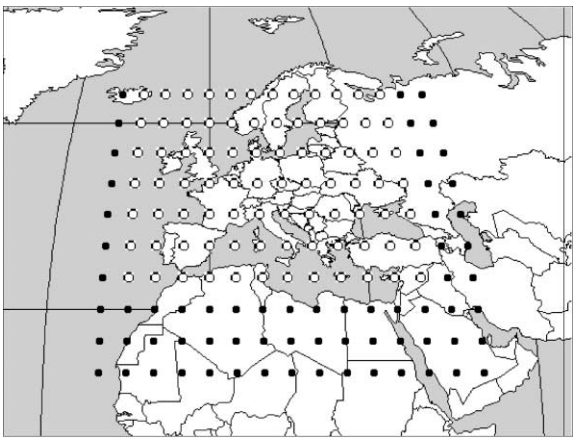

Fig. 3. Two pressure widows used for CPs optimization: German (white) and Greek (black) in $5 \times 5^{\circ}$ resolution.

where the frequency ω is $2\pi/365$. The advantage of Fourier series approximation (instead of simple polynomial fit) is that adding new A_k and B_k parameters do not change the values of the former ones. For $K = 182$ the Fourier approximation is identical with the observed series. Usually the first three Fourier parameters are enough to simulate the annual cycle of autocorrelation. The annual cycle of autocorrelation was computed by means of 45-day moving window.

The proportion of variance accounted for by each harmonic can be computed as follows:

$$R_k^2 = \frac{n/2(a_k^2 + b_k^2)}{(n-1)s^2} \tag{9}$$

where s^2 is the sample variance of the series. Since each harmonic provides independent information about the data series, the joint proportion of variance exhibited by a regression equation with only harmonic predictors is the sum of the R_k^2 values for each of the harmonics (for maximum number (n/2) of harmonics the sum of R_k^2 is 1).

The $\mathbf{C}_i(t^*)$ matrix takes spatial variability of the process into account. This $n \times n$ matrix is related to $\mathbf{W}(t)$ through (Bras and Rodriguez-Iturbe, 1985 in p. 93):

$$\Gamma_{0i}(t^*) = E\Big[(\mathbf{W}(t) - \mathbf{w}_i(t^*))(\mathbf{W}^{\mathrm{T}}(t) - \mathbf{w}_i^{\mathrm{T}}(t^*))\Big] \tag{10}$$

$$\Gamma_{1i}^{\mathrm{T}}(t^*) = E\Big[(\mathbf{W}(t-1) - \mathbf{w}_i(t^*-1))(\mathbf{W}^{\mathrm{T}}(t) - \mathbf{w}_i^{\mathrm{T}}(t^*))\Big] \tag{11}$$

$$\mathbf{C}_i(t^*)\mathbf{C}_i^{\mathrm{T}}(t^*) = \mathbf{\Gamma}_{0i}(t^*) - \mathbf{\Gamma}_{1i}(t^*)\mathbf{\Gamma}_{0i}^{-1}(t^*)\mathbf{\Gamma}_{1i}^{\mathrm{T}}(t^*) \tag{12}$$

where $\mathbf{\Gamma}_{0i}(t^*)$ is the spatial covariance matrix and $\mathbf{\Gamma}_{1i}(t^*)$ is the space-time covariance matrix for the time lag of one day. Assuming that these two matrices are related to each other through:

$$r(t^*)\mathbf{\Gamma}_{0i}(t^*) = \mathbf{\Gamma}_{1i}(t^*) \tag{13}$$

leads to

$$\mathbf{C}_i(t^*)\mathbf{C}_i^{\mathrm{T}}(t^*) = (1 - r^2(t^*))\mathbf{\Gamma}_{0i}(t^*) \tag{14}$$

Table 1
CP and precipitation characteristics at station Stuttgart. Values in the table are averaged over the period 1970–1990

CP	CP occurrence frequency (%)					Precipitation probability (%)					Mean wet-day amount (mm)				
	Spring	Summer	Fall	Winter	Year	Spring	Summer	Fall	Winter	Year	Spring	Summer	Fall	Winter	Year
1	35.2	45.2	40.5	39.7	40.2	26.9	30.5	18.4	26.3	25.6	1.0	2.1	0.7	0.5	1.1
2	11.3	5.4	7.0	12.1	9.0	46.2	56.0	42.2	30.3	41.5	2.5	4.3	1.5	0.7	2.0
3	7.9	4.6	8.0	11.3	7.9	67.1	64.3	74.0	62.7	66.9	2.6	3.9	3.4	2.3	2.9
4	2.5	2.8	3.1	2.7	2.8	60.9	38.5	53.6	54.2	51.5	2.0	0.7	2.2	1.3	1.5
5	3.6	3.0	3.4	5.1	3.8	36.4	39.3	48.4	41.3	41.3	1.5	2.0	1.4	1.3	1.5
6	4.9	5.1	5.1	3.3	4.6	33.3	14.9	26.1	33.3	26.2	2.4	1.3	1.1	1.1	1.5
7	0.8	1.7	1.8	1.4	1.4	71.4	75.0	56.3	46.2	61.5	0.8	3.0	0.9	1.3	1.6
8	10.9	10.4	13.4	8.2	10.7	68.0	67.7	76.2	82.4	73.2	2.1	3.3	3.4	1.8	2.8
9	8.0	6.0	4.2	5.7	6.0	63.5	65.5	68.4	70.6	66.5	2.6	3.6	2.1	2.8	2.8
10	5.8	7.1	5.4	4.3	5.6	43.4	29.2	34.7	69.2	41.7	0.9	1.7	1.8	1.8	1.5
11	4.9	4.1	3.0	2.8	3.7	57.8	71.1	66.7	32.0	58.5	2.2	3.1	2.8	0.4	2.2
12	2.7	3.3	3.3	1.7	2.7	48.0	56.7	73.3	73.3	62.0	1.5	3.2	2.0	1.3	2.2

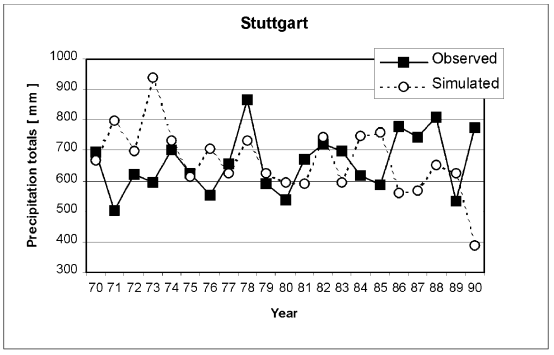

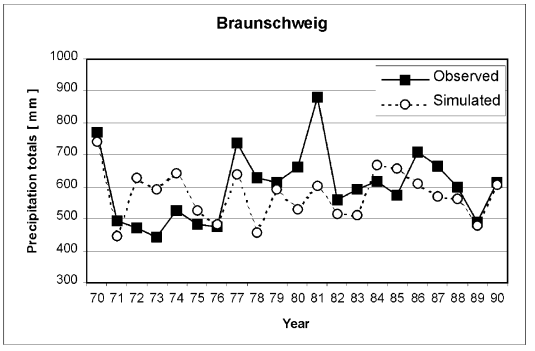

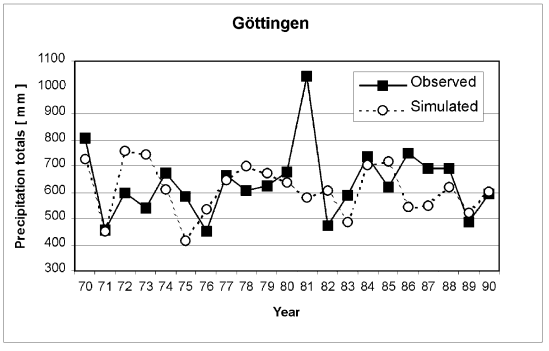

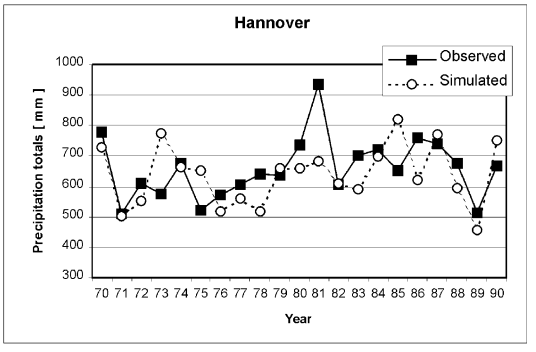

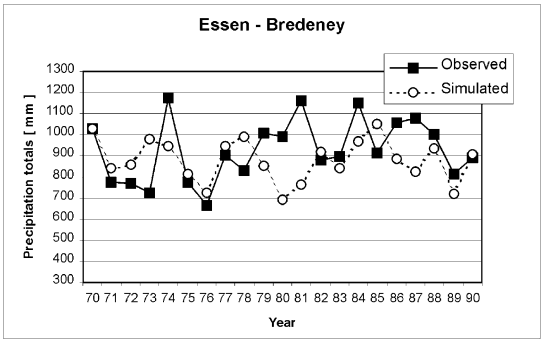

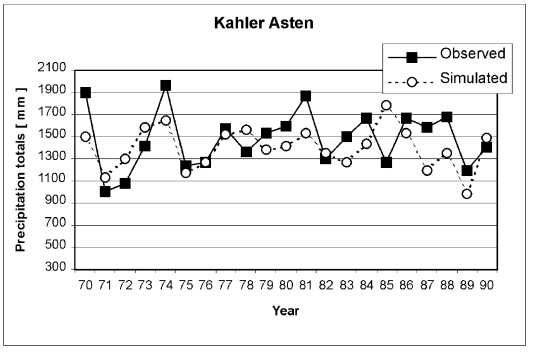

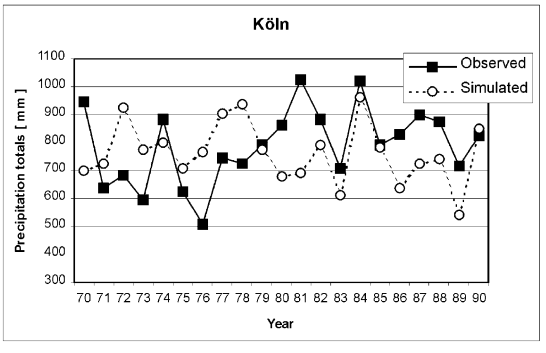

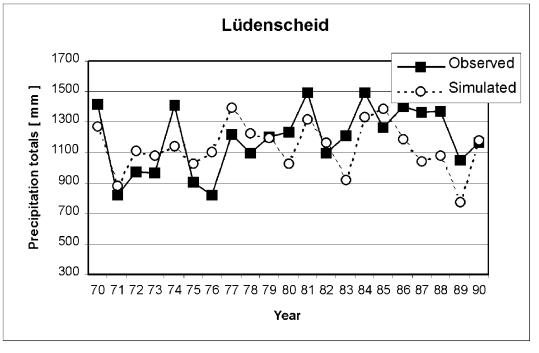

Fig. 4. Annual precipitation totals for observed and simulated series at eight stations in Germany.

The decomposition of $\mathbf{C}_i(t^*)\mathbf{C}_i^{\mathrm{T}}(t^*)$ is in detail described in Bárdossy and Plate (1992). Another method which could be applied is proposed by Koutsoyiannis (1999). Eq. (1) establishes the link between $\mathbf{W}(t)$ and the rainfall $\mathbf{Z}(t)$; thus the multisite process is fully described.

2.2.2. Parameter estimation

The temporal parameters are computing by means of maximum likelihood method. Assuming that parameters of the precipitation annual cycle depend on the CP i and time of the year t^* one has:

$$w_i(t^*,u) = \frac{a_0(w_i,u)}{2} + \sum_{k=1}^{K}(a_k(w_i,u)\cos(k\omega t^*) + b_k(w_i,u)\sin(k\omega t^*)) \quad (15)$$

$$\sigma_i(t^*,u) = \frac{c_0(\sigma_i,u)}{2} + \sum_{k=1}^{K}(c_k(\sigma_i,u)\cos(k\omega t^*) + d_k(\sigma_i,u)\sin(k\omega t^*)) \quad (16)$$

where $\sigma_i(t^*,u)$ is the standard deviation of the transformed precipitation amount $W(t,u)$ on Julian date t^*. $\sigma_i(t^*,u)$ is connected with $\mathbf{\Gamma}_{0i}(t^*)$ as it contains the variances in its main diagonal. Due to this fact the correlations are used for the estimation of the spatial covariances.

The log-likelihood function can be written following the derivation of Henze and Klar (1993)

$$L(w_i(t^*,u),\sigma_i(t^*,u);Z(t,u),t=1,\ldots,T) = \sum_{Z(t,u)=0}\log\Phi\left(\frac{-w_i(t^*,u)}{\sigma_i(t^*,u)}\right) + \sum_{Z(t,u)>0} \times\log\left[\frac{Z(t,u)^{(1/\beta)-1}}{\beta\sigma_i(t^*,u)}\phi\left(\frac{Z(t,u)^{1/\beta}-w_i(t^*,u)}{\sigma_i(t^*,u)}\right)\right] \quad (17)$$

where ϕ and Φ denote the density function and the cumulative distribution function of the standard normal distribution respectively.

This equation can be simplified to:

$$L(\cdot) = \sum_{Z(t,u)=0}\log\Phi\left(\frac{-w_i(t^*,u)}{\sigma_i(t^*,u)}\right) + \sum_{Z(t,u)>0}\log\sigma_i(t^*,u) - \sum_{Z(t,u)>0}\log\beta + \left(\frac{1}{\beta}-1\right)\sum_{Z(t,u)>0}\log Z(t,u) - \frac{1}{2}\sum_{Z(t,u)>0}\log(2\pi) + \frac{1}{2}\sum_{Z(t,u)>0}\left(\frac{Z(t,u)^{1/\beta}-w_i(t^*,u)}{\sigma_i(t^*,u)}\right)^2 \quad (18)$$

Summing the terms which do not depend on the Fourier coefficients to K one has:

$$L(\cdot) = K + \sum_{Z(t,u)=0}\log\Phi\left(\frac{-w_i(t^*,u)}{\sigma_i(t^*,u)}\right) + \sum_{Z(t,u)>0}\log\sigma_i(t^*,u) + \frac{1}{2}\sum_{Z(t,u)>0}\left(\frac{Z(t,u)^{1/\beta}-w_i(t^*,u)}{\sigma_i(t^*,u)}\right)^2 \quad (19)$$

The above function has to be maximized as a function of $a_0(w_i,u),\ldots,a_K(w_i,u)$, $b_1(w_i,u),\ldots,b_K(w_i,u)$, $c_0(\sigma_i,u),\ldots,c_K(\sigma_i,u)$, $d_0(\sigma_i,u),\ldots,d_K(\sigma_i,u)$. This can be done by numerical optimization using appropriate algorithms. The convergence can be substantially increased by using the first approximation for $w_i(t^*,u)$ and $\sigma_i(t^*,u)$ for a selected set of points (for example 12 mid days of the 12 months)

Table 2
Statistics of observed and simulated annual totals 1970–1990, eight stations in Germany

Station	Mean		Standard deviation	
	Observed	Simulated	Observed	Simulated
Stuttgart	661	665	98	111
Braunscweig	600	574	112	77
Göttingen	636	612	134	97
Hannover	658	637	101	99
Essen-Bredeney	928	881	148	101
Kahler Asten	1481	1401	263	190
Köln	790	763	137	109
Lüdenscheid	1190	1135	211	161

Table 3
Correlation between spatial patterns of observed and simulated yearly totals 1970–1990, eight stations in Germany

Year	1970	1971	1972	1973	1974	1975	1976	1977	1978	1979	1980
r	0.97	0.90	0.94	0.97	0.99	0.92	0.91	0.96	0.92	0.98	0.96
Year	1981	1982	1983	1984	1985	1986	1987	1988	1989	1990	
r	0.95	0.97	0.98	0.98	0.95	0.99	0.96	0.99	0.93	0.91	

and then fitting initial $a_0(w_i,u),\ldots,a_K(w_i,u)$, $b_1(w_i,u),\ldots,b_K(w_i,u)$, $c_0(\sigma_i,u),\ldots,c_K(\sigma_i,u)$, $d_0(\sigma_i,u),\ldots,d_K(\sigma_i,u)$. Starting from this point ensures a quick optimization. The optimization of the Fourier parameters of the autocorrelation function described by the Eq. (8) is done by the same technique.

The spatial structure of the rainfall is described using a circulation pattern dependent covariance structure of the matrix $\mathbf{\Gamma}_{0i}(t^*)$ and $\mathbf{\Gamma}_{1i}(t^*)$. The covariance structure is assumed to be translation invariant but time dependent supposing:

$$\mathrm{cov}[Z_x, Z_y]_i(t) = p_i(t^*)\,\mathrm{e}^{-h(x,y)q_i(t^*)} \tag{20}$$

where h is distance. The parameters p_i and q_i depend on the circulation pattern i and the time of the year and are also modeled by means of Fourier series. Anisotropy is taken into account by introducing a coordinate transformation

$$x' = \lambda(x\cos\gamma + y\sin\gamma) \tag{21}$$

$$y' = -x\sin\gamma + y\sin\gamma \tag{22}$$

where (x,y) are the coordinates in the original and (x',y') those in the transformed system, γ is the rotation angle and λ is the ratio of two orthogonal ranges representing the highest and the lowest variability. It is supposed that the anisotropy changes with the circulation pattern but for a given circulation pattern remains constant during the year (due to flow direction). The parameters of the spatial correlation funtion including λ and γ are estimated using a least squares approach. The generating of precipitation series is based on the Eq. (6). The series are generated day by day for a set of points simultaneously. For a given series of CPs the corresponding precipitation is generated using a randomly generated $\mathbf{\Psi}(t)$ and the values of the previous day in Eq. (6). It is an advantage of the presented model that it takes the spatial correlation among precipitation series into account. Therefore it is suitable also for generating of areal precipitation. In both presented case studies, the parameters of the downscaling model as well as the daily series of CPs were known. However, for generating very long precipitation series also the series of CPs should be generated. One possibility how to generate the CPs series based on the semi-Markov chains was introduced by Bárdossy and Plate (1991).

The present model is an advancement of the precipitation model developed by Bárdossy and Plate (1992). This model included winter and summer seasons, where the new model includes the annual cycle and generates precipitation time series for several sites. Now it is possible to simulate precipitation for a set of points simultaneously. Further the annual cycle of spatial covariances was introduced and the parameter estimation is improved.

3. Application

In order to test the downscaling model under different climate conditions, it was applied in two regions in Europe, namely in Central Europe (eight stations in Germany) and Eastern Mediterranean (21 stations in Greece). The locations of Greek and German stations are shown in Figs. 1 and 2. For the German stations the average monthly amounts are mostly more or less comparable during the year or they reveal maximum during the summer months. However, for the most Greek stations a pronounced precipitation cycle with almost no rain in summer is typical. Also there are great differences of precipitation measurements at different stations at the same day. It happens that one station might measure high rainfall amounts while no rainfall is recorded in some others.

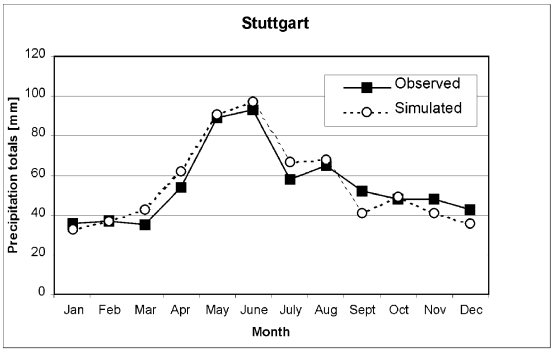

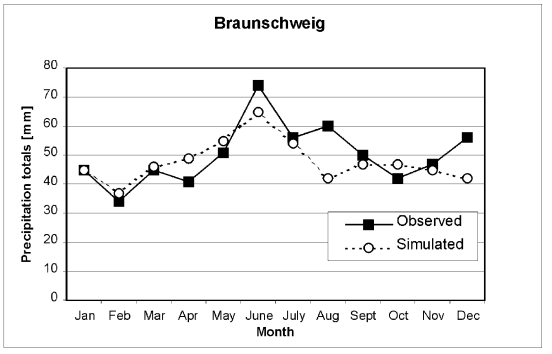

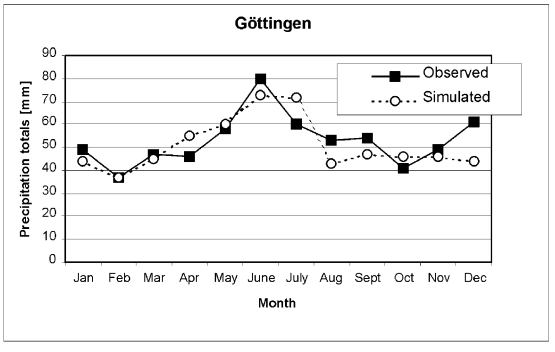

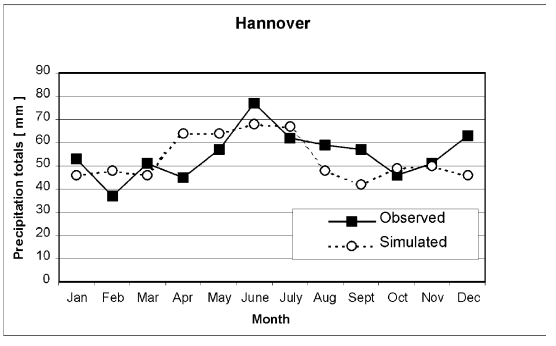

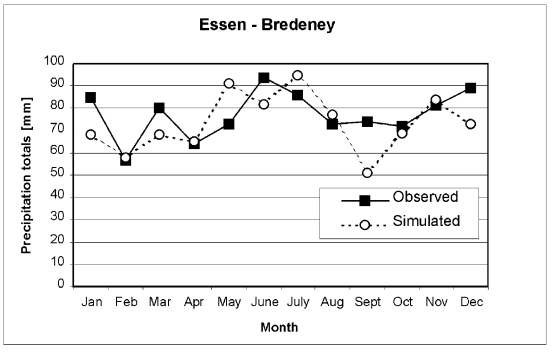

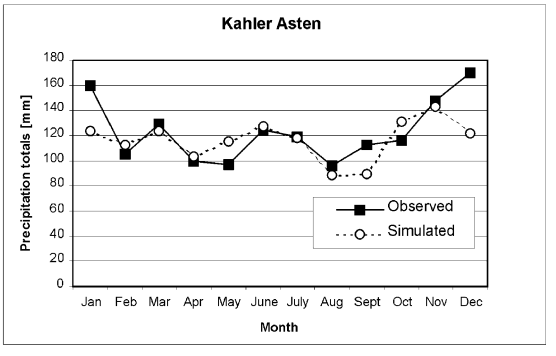

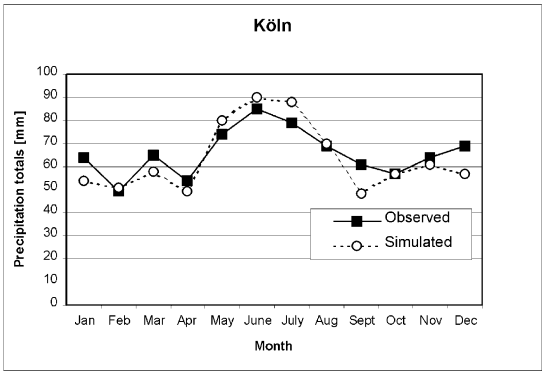

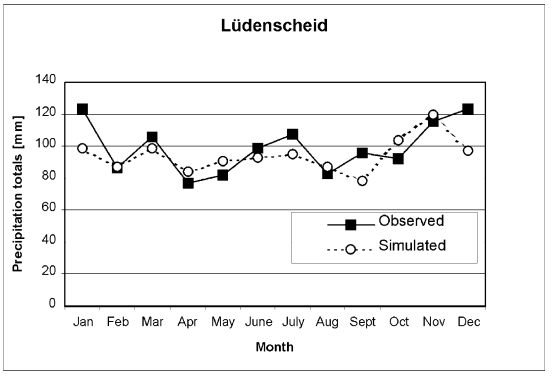

Fig. 5. Average annual cycles of precipitation for observed and simulated series in Germany (1970–1990).

Table 4
Correlations between observed and simulated monthly totals in the average annual cycle 1970–1990, German stations (Fig. 5)

Station	r
Stuttgart	0.96
Braunschweig	0.67
Göttingen	0.74
Hannover	0.39
Essen-Bredeney	0.49
Kahler Asten	0.59
Köln	0.90
Lüdenscheid	0.58

3.1. Results for Germany/Central Europe

The classification of daily circulation patterns is based on 500 hPa geopotential height data in the space window 35°N–65°N, 15°W–40°E (Fig. 3). The data comes from the National Meteorological Centre for Atmospheric Research (NCAR) and the National Meteorological Centre (NMC). The grid resolution is $5° \times 5°$. Twelve circulation patterns were defined based on the automated objective optimization procedure, which is focused on explaining variability of precipitation behavior at the same stations used for downscaling. The results of circulation patterns classifications are detailed described in Bárdossy et al. (2001). Table 1 presents CPs and precipitation characteristics for station Stuttgart. The average occurrence frequency of most CPs is approximately the same in each season; an exception is, for example CP 3, with 4.6% of occurrence in summer and 11.3% in winter. Generally, it holds that — comparing to other CPs — wettest CPs are wet and driest CPs are dry in every season.

For calibration and validation of the downscaling model the observed and simulated daily precipitation amounts from eight precipitation stations spread over Germany were used. The model was calibrated in 1970–1979, validated in 1980–1990 and applied for the whole period 1970–1990.

Graphs of observed and modeled cycles of annual totals are presented in Fig. 4. Because of the statistical character of the modeling the simulated totals often differ from the observed ones and the correlations at each site are not too high. However, more important is

Table 5
Precipitation diagnostics according to Wilby et al. (1998b) for the stations Stuttgart, Köln and Kahler Asten for the validation period 1970–1990. Comparison of observed and simulated precipitation series

Diagnostic	Unit	Stuttgart (315 m asl)		Köln (92 m asl)		Kahler Asten (839 m asl)	
		Observed	Simulated	Observed	Simulated	Observed	Simulated
Mean wet-day amount (>0.05 mm)	(mm)	4.01	4.73	4.10	4.60	6.26	6.91
Standard deviation of wet-day amount	(mm)	5.89	6.00	5.34	5.54	7.83	7.64
Median wet-day amount	(mm)	2.00	2.60	2.20	2.70	3.30	4.40
P_{00} dry-day probability conditional on previous day being dry	[ ]	0.38	0.46	0.32	0.38	0.22	0.29
P_{11} wet-day probability conditional on previous day being wet	[ ]	0.29	0.23	0.38	0.29	0.52	0.39
π_W unconditional probability of a wet-day	[ ]	0.45	0.39	0.53	0.45	0.65	0.55
L_w mean wet-spell length	(day)	2.74	2.41	3.54	2.75	4.90	3.46
L_d mean dry-spell length	(day)	3.34	3.85	3.16	3.31	2.67	2.78
Number of dry spells >10 days in vegetation period (April–September)	[ ]	21.00	38.00	26.00	30.00	10.00	15.00
Standard deviation of monthly precipitation total	(mm)	32.97	39.2	34.27	38.3	67.82	57.93
R_x maximum daily precipitation	(mm)	96.90	59.00	57.90	51.00	62.90	66.30

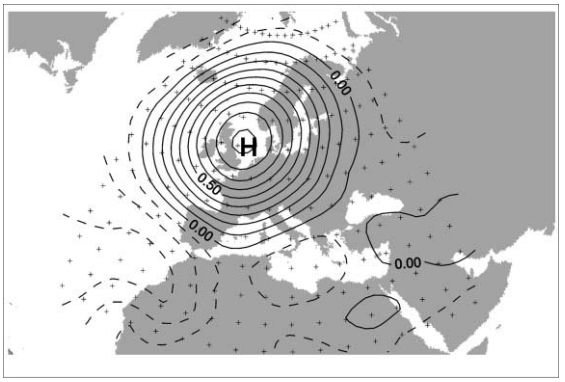

Fig. 6. Mean normalized distributions of 500 hPa geopotential height anomalies for CP 1, averaged over 1970–1979.

that the simulation results are very good from the mean value and variance point of view (Table 2).

In spite of the relatively high difference between observed and modeled annual totals, the spatial patterns of these totals are highly correlated: the correlation coefficient between observed and modeled annual precipitation totals for all eight stations is at least 0.9 (Table 3). The annual cycles are reproduced very well (Fig. 5). Very good agreements were achieved both for stations with pronounced maximum in summer (like Stuttgart) and for stations with the winter maximum (e.g. Kahler Asten). In some cases the simulated precipitation totals for December and January are a little bit underestimated (Essen Bredeney, Kahler Asten, Köln, Lüdenscheid). The correlations at each site are reported in Table 4. They are

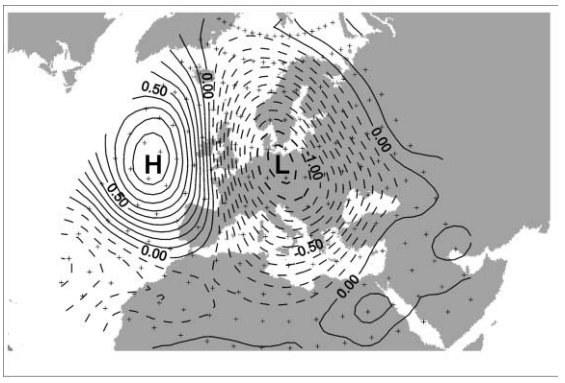

Fig. 7. Mean normalized distributions of 500 hPa geopotential height anomalies for CP 8, averaged over 1970–1979.

higher for stations with pronounced cycle (e.g. Stuttgart) and lower for stations having more smooth cycle (e.g. Lüdenscheid).

For the need of comparison between observed and simulated precipitation series the standard diagnostics according to Wilby et al. (1998b) was applied. In Table 5, the diagnostics is presented for three stations with different elevations. It shows that in general the simulations slightly overestimate the amount of rainfall on rainy days. The reason for this is that the model was developed with special emphasis on the reproduction of extreme rainfall events (the objective function of the classification enables to take precipitation amounts above a certain threshold into account) and therefore tends to overestimate rainfall amounts. The standard deviations of wet day amount are reproduced very well. The unconditional probability of a wet day and the conditional probabilities P_{00} and P_{11} yield comparable values both for observed and simulated series. Also the reproduction of the mean spell lengths is quite well, only the long dry-day periods during the vegetation period are somewhat overestimated. Table 5 shows also that standard deviations of monthly precipitation totals are comparable. Even such values like maximum daily precipitation are reproduced very well. There is no systematic over- or underestimation. Thus applicability of the model is proved.

Because the precipitation model is based on the CP-conditioned concept, two examples of CPs resulting from the objective classification are given. Figs. 6 and

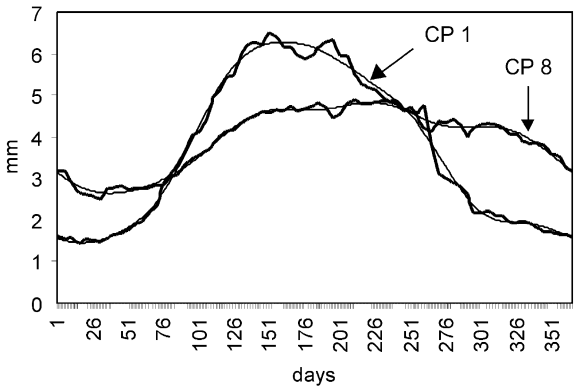

Fig. 8. Annual cycle of precipitation conditioned to occurence of CP 1 and CP 8: comparison between observed data (thick line) and Fourier approximation (thin line) by three harmonics for the station Stuttgart (1970–1990).

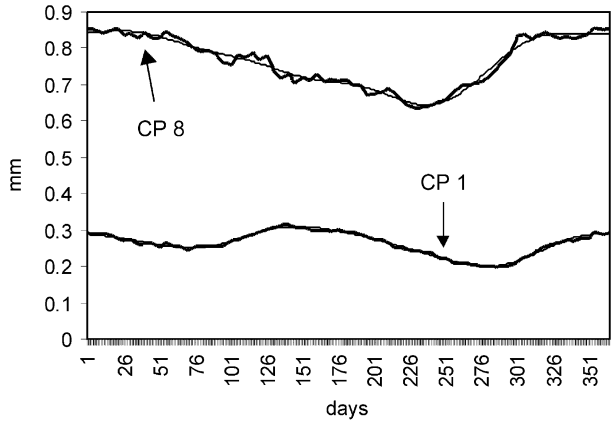

Fig. 9. Annual cycle of precipitation probability conditioned to occurence of CP 1 and CP 8: comparison between observed data (thick line) and Fourier approximation (thin line) by three harmonics for the station Stuttgart (1970–1990).

Table 6
Explained variance for precipitation and precipitation probability by each from the first three Fourier harmonics and their sum

Number of harmonics	German stations		Greek stations	
	Precipitation	Precipitation probability	Precipitation	Precipitation probability
1	64.45	62.78	58.09	87.28
2	20.01	20.78	21.69	7.00
3	6.98	6.91	8.61	2.45
Sum	91.44	90.56	88.39	96.73

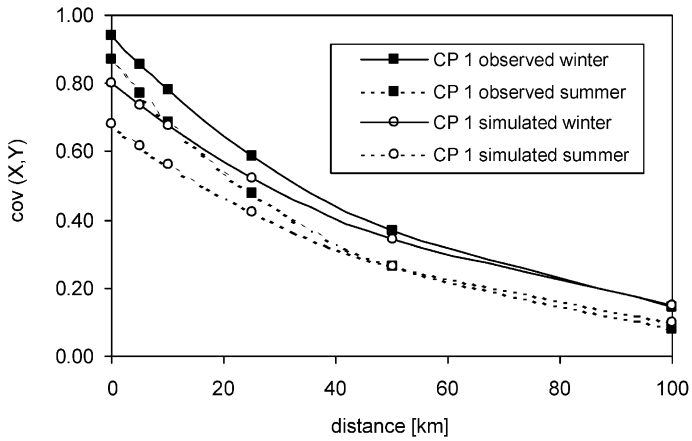

Fig. 10. Spatial covariance functions for CP 1 in winter and in summer for observed and simulated series.

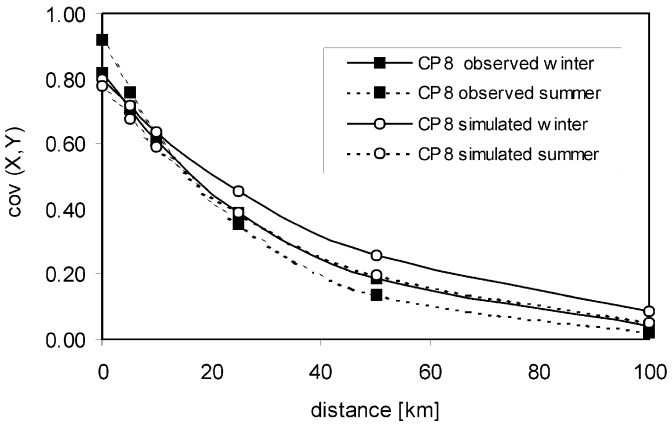

Fig. 11. Spatial covariance functions for CP 8 in winter and in summer for observed and simulated series.

7 show the distributions of mean (1970–1979) normalized 500 hPa pressure anomalies for one dry (CP 1) and one wet (CP 8) circulation pattern. CP 1 has very low precipitation probability (25.6%), mean wet-day amount (1.1 mm) and wetness index (0.63). This index is computed as ratio between precipitation contribution and occurrence frequency of each CP and its low value means that CP 1 contributes only very little to rainfall. The map shows that the CP 1 is characterized by pronounced high-pressure anomaly east of British Isles, which causes a weak air movement and transport of dry air masses from northeastern Europe to central European. On the other hand CP 8 is a typical wet CP with high precipitation probability (84.1%), mean wet-day amount (4.1 mm) and wetness index (2.1). The map shows that eastern position of low-pressure anomaly and western position of higher anomaly result in transport of wet air from the North sea. The maps of pressure anomalies prove that the automated classification method produces physically realistic results.

CP-conditioned annual cycles of precipitation and its probability of occurrence for both above described CPs are presented in Figs. 8 and 9. CP-conditioned annual cycles of precipitation differ substantially from each other (Fig. 8). Whereas CP 1-conditioned cycle has distinct maximum in summer, the cycle belonging to CP 8 is much smoother. In Fig. 8 the Fourier series of three harmonics for each precipitation cycle is also presented. The agreement between each pair of lines

Table 7
CP and precipitation characteristics at station Athens. Values in the table are averaged over the period 1970–90

CP	CP occurrence frequency (%)					Precipitation probability (%)					Mean wet-day amount (mm)				
	Spring	Summer	Fall	Winter	Year	Spring	Summer	Fall	Winter	Year	Spring	Summer	Fall	Winter	Year
1	9.57	8.70	7.47	10.11	8.95	47.73	17.50	48.53	61.54	44.34	2.96	0.69	5.30	6.38	3.84
2	8.26	7.07	8.13	10.33	8.43	40.79	12.31	21.62	44.09	31.17	1.01	0.36	1.59	2.29	1.40
3	5.54	6.74	10.77	8.22	7.80	21.57	3.23	22.45	24.32	18.60	1.22	0.04	0.62	1.25	0.77
4	7.72	8.15	7.91	6.67	7.64	18.31	4.00	23.61	33.33	19.00	0.43	0.02	1.46	1.43	0.80
5	4.67	5.98	4.73	4.44	4.96	27.91	7.27	25.58	32.50	22.10	1.13	0.58	3.85	0.68	1.51
6	2.17	1.63	1.21	2.00	1.75	10.00	0.00	9.09	50.00	18.75	0.63	0.00	0.45	2.39	0.95
7	5.43	5.33	5.05	3.78	4.90	14.00	0.00	26.09	35.29	17.32	0.30	0.00	0.82	3.04	0.87
8	3.70	3.48	3.63	4.44	3.81	23.53	3.13	15.15	27.50	17.99	0.64	0.05	0.69	0.81	0.57
9	31.30	30.33	32.31	30.22	31.05	6.60	1.08	2.72	14.34	6.08	0.13	0.02	0.26	0.55	0.24
10	8.91	9.13	6.26	6.22	7.64	32.93	11.90	52.63	55.36	35.13	1.68	0.43	3.65	3.97	2.16
11	7.93	8.26	6.04	9.33	7.89	9.59	2.63	7.27	19.05	10.07	0.15	0.12	0.55	0.64	0.36
12	3.15	4.35	3.41	3.00	3.48	24.14	5.00	29.03	48.15	24.41	0.70	0.35	0.73	2.56	0.99

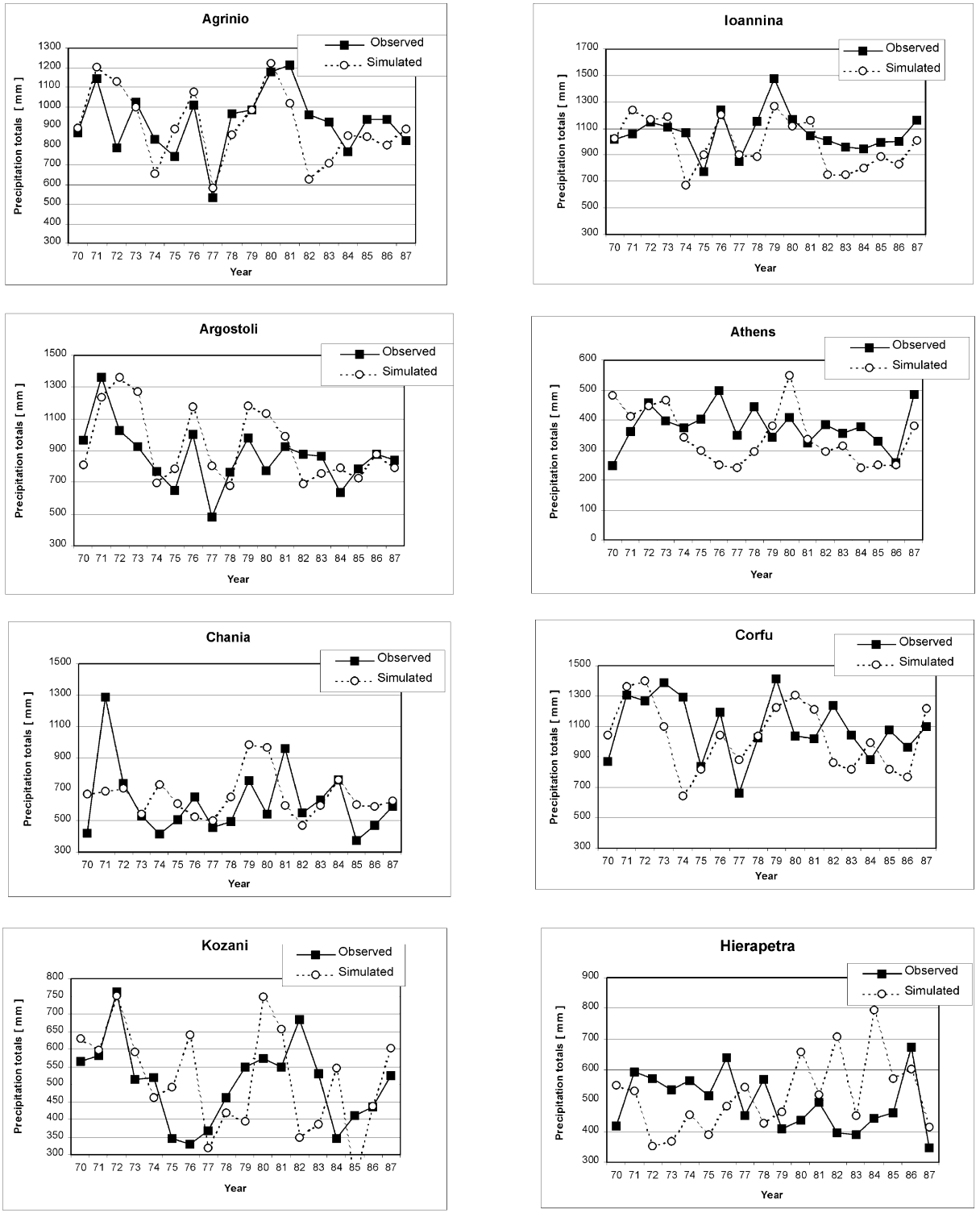

Fig. 12. Annual precipitation totals for observed and simulated series at eight stations in Greece.

Table 8
Statistics of observed and simulated annual totals 1970–1987, 21 stations in Greece

Station	Mean		Standard deviation	
	Observed	Simulated	Observed	Simulated
Agrinio	875	854	166	187
Alexandroupoli	502	489	124	141
Argostoli	815	883	188	231
Athens National Obs.	358	328	68	94
Chania	586	622	224	139
Corfu	1032	976	205	222
Heraklio	463	490	118	155
Hierapetra	469	489	93	119
Ioannina	1009	936	154	189
Kalamata	764	722	137	152
Kozani	476	487	117	150
Kythira	497	490	94	132
Larissa	419	397	116	115
Milos	389	386	74	93
Mytilene	642	610	124	119
Naxos	389	365	115	88
Rhodes	612	638	120	154
Samos	725	711	171	170
Skyros	422	435	150	124
Thessaloniki	448	418	106	104
Tripoli	765	723	133	150

proves that the Fourier series yields very good approximation of the observed data. Annual cycles of precipitation probability and their Fourier approximations are given in Fig. 9. These lines are very smooth; however, the precipitation probability conditioned to occurrence of CP 8 is up to three times higher than this for CP 1.

According to Eq. (9) the proportion of variance of CP-conditioned annual cycle of precipitation and precipitation probability for each station and each CP was computed. The results are shown in Table 6 where a mean value for each from three computed harmonics is presented. From the Table 6 follows that most of the variation in the precipitation data is described by the first harmonics, the R^2 for which is 64.45%. The first three harmonics account for (in average) 91.44% of variance of CP-conditioned precipitation annual cycle. This fact proves the suitability of the Fourier transform approximation. Similar results were obtained for precipitation probability.

Annual cycle of autocorrelation for observed as well as simulated series is weakly pronounced with slightly lower autocorrelations in summer than in winter. Taking into account the fact that winter rainfall is mostly caused by cyclonic atmospheric conditions at the large-scale, whereas, summer rains are often produced by local convective systems, such a result is not surprising.

Spatial covariance functions for both CP 1 and CP 8 for summer and winter season and for observed and

Table 9
Correlation between spatial patterns of observed and simulated annual totals 1970–1987, 21 stations in Greece

year	1970	1971	1972	1973	1974	1975	1976	1977	1978	1979	1980
r	0.80	0.87	0.86	0.89	0.60	0.70	0.80	0.58	0.85	0.88	0.86
Year	1981	1982	1983	1984	1985	1986	1987				
r	0.78	0.56	0.89	0.79	0.73	0.78	0.82				

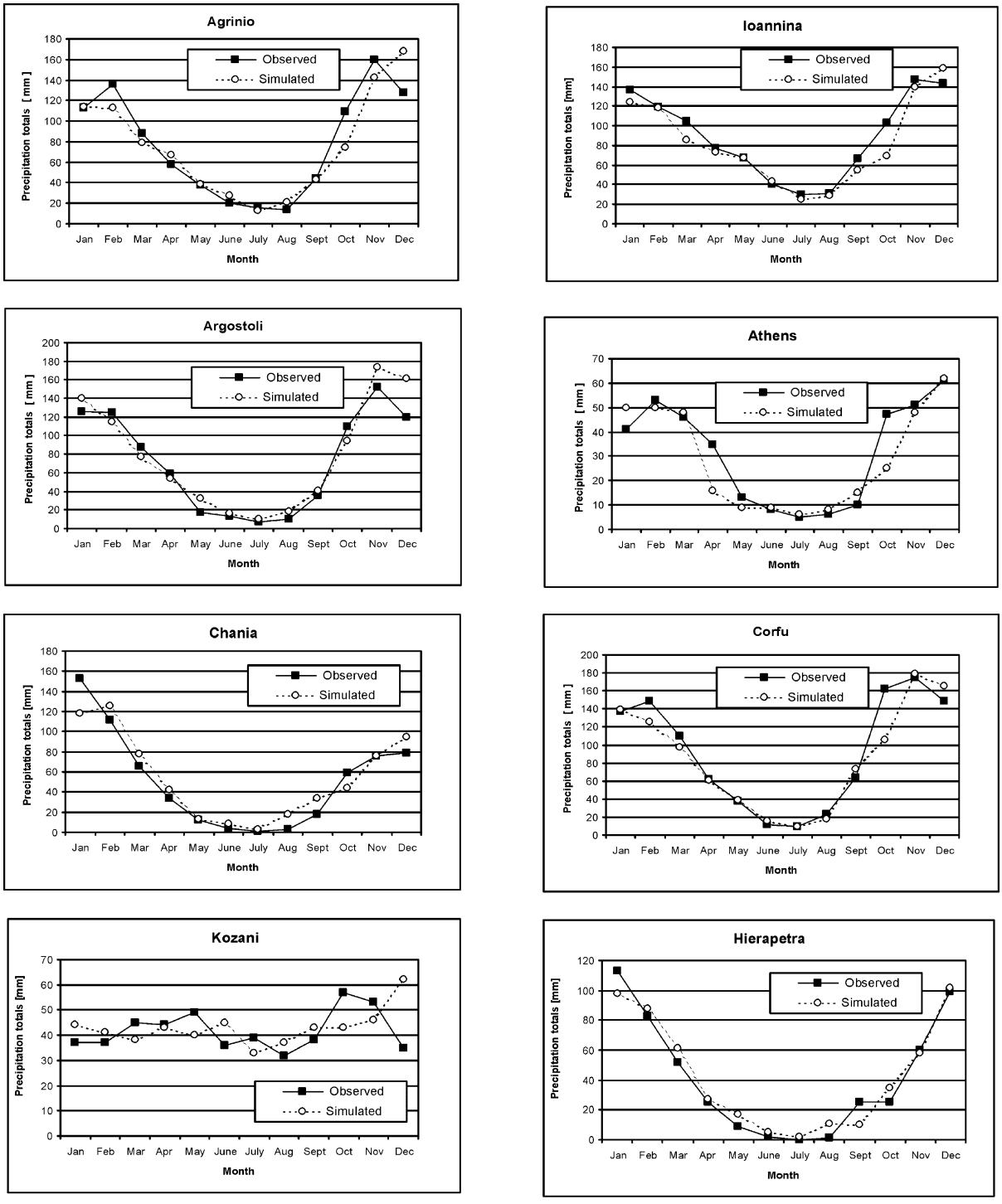

Fig. 13. Average annual cycles of precipitation for observed and simulated series in Greece (1970–1987).

Table 10
Precipitation diagnostics according to Wilby et al. (1998b) for the stations Agrinio, Corfu and Kozani for the validation period 1970–1987. Comparison of observed and simulated precipitation series

Diagnostic	Unit	Agrinio (47 m asl)		Corfu (4 m asl)		Kozani (627 m asl)	
		Observed	Simulated	Observed	Simulated	Observed	Simulated
Mean wet-day amount (>0.05 mm)	(mm)	9.28	9.88	10.11	10.58	5.37	6.03
Standard deviation of wet-day amount	(mm)	13.05	12.17	14.02	13.00	7.49	8.41
Median wet-day amount	(mm)	4.90	5.40	4.70	6.00	2.80	3.10
P_{00} dry-day probability conditional on previous day being dry	[ ]	0.61	0.62	0.59	0.61	0.61	0.63
P_{11} wet-day probability conditional on previous day being wet	[ ]	0.15	0.12	0.18	0.14	0.13	0.10
π_W unconditional probability of a wet-day	[ ]	0.27	0.25	0.30	0.27	0.26	0.23
L_w mean wet-spell length	(day)	2.26	1.96	2.52	2.10	1.96	1.76
L_d mean dry-spell length	(day)	6.03	5.88	6.00	5.79	5.67	5.77
Number of dry-spells >10 days in vegetation period (April–September)	[ ]	68.00	83.00	79.00	90.00	80.00	76.00
Standard deviation of monthly precipitation total	(mm)	72.37	75.87	86.16	85.92	31.53	36.31
R_x maximum daily precipitation	(mm)	171.70	87.30	129.10	113.90	95.80	112.90

simulated series, respectively, are shown in Figs. 10 and 11. In all the cases, a clear spatial dependence could be observed with a slow decrease of the covariance with increasing distance between the stations.

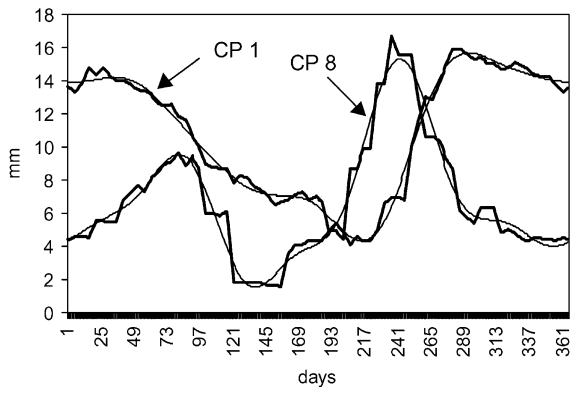

Fig. 14. Annual cycle of precipitation conditioned to occurrence of CP 1 and CP 8: comparison between observed data and Fourier approximation by three harmonics for the station Agrinio (1970–1987).

For both CPs (with the exception of CP 8-conditioned observed series in summer for short distances) the covariance functions in the same distance are for summer lower than for winter. This fact proves lower spatial persistence of summer rainfall events in comparison to the winter ones. The cause is probably that the summer rainfall is often produced by small-scale convective events whereas winter rainfall is associated with low-pressure anomalies at larger scale as discussed above in case of annual cycle of autocorrelation. When comparing the covariance functions for simulated series with those for observed series it is obvious that in case of CP 1 the simulated series slightly underestimate spatial covariances for shorter distances. On the other hand, for CP 8 the covariances of simulated series are a little bit overestimated with the exception of very short distances (up to 10 km) for summer series.

3.2. Results for Greece/Eastern Mediterranean

For circulation patterns classification the 700 hPa

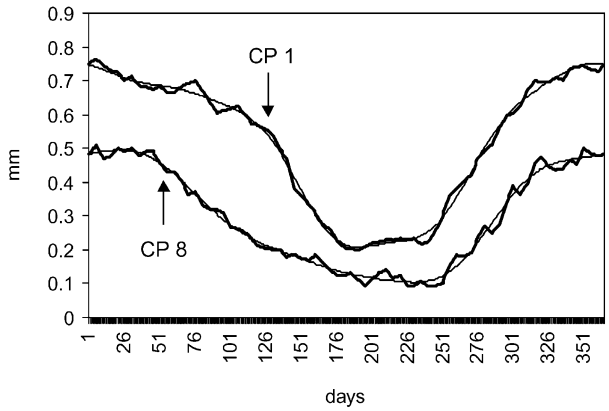

Fig. 15. Annual cycle of precipitation probability conditioned to occurrence of CP 1 and CP 8: comparison between observed data and Fourier approximation by three harmonics for the station Agrinio (1970–1987).

pressure data in the window 20°N–65°N, 20°W–50°E were used (Fig. 3). Again 12 circulation patterns were defined which account for the variability of precipitation behavior of selected Greek stations. CPs and precipitation statistics for the precipitation station Athens which is placed approximately in the middle of the investigated area and has a typical annual cycle of precipitation with very little precipitation in summer and higher precipitation in winter is shown in Table 7. From the table it follows that CP 6 and CP 7 do not contribute to summer precipitation at all, because of the precipitation probability being nearly 0. As in the case of the German study the occurrence frequency of most CPs remains approximately the same in each season. Whereas other CPs have frequency between 2 and 10%, CP 9 is exceptionally frequent occurring in approximately 30% of the days in each season. For Athens very wet and very dry CPs have wet or dry character in every season.

For the comparison between observed and simulated precipitation series the time period 1970–1987 was considered. Graphs of annual precipitation totals both for observed and simulated series are shown in Fig. 12. Like in the case of Germany the statistical CP-conditioning results in differences between observed and simulated amounts in a concrete year. However, the mean values and variability of both series are comparable (Table 8).

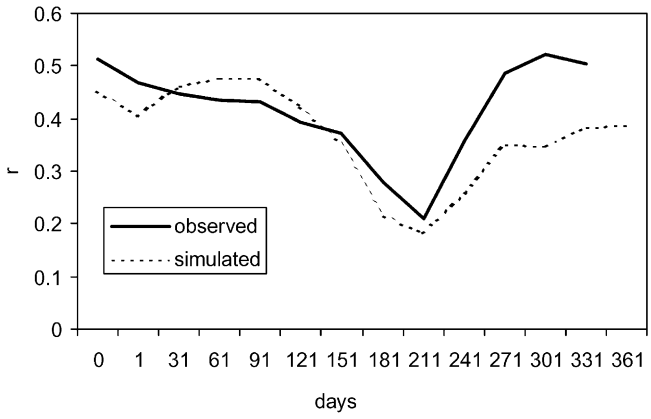

Fig. 16. Average annual cycle of lag 1 autocorrelation of daily precipitation for observed and simulated precipitation series (21 Greek stations, 1970–1987).

Because of high spatial variability of precipitation under Greek climate conditions the correlation coefficients between observed and simulated spatial patterns of annual precipitation totals for all 21 stations are not so high as for German stations. The stochastic character of the modeling leads to relatively low correlations in some years (like 1972, 1977 and 1982). However, the correlations are in average 0.78 (Table 9). Concerning the seasonal cycle of precipitation the simulation results are very good especially for stations having typical pronounced cycle with almost no precipitation in summer (Fig. 13). The correlation coefficient between observed and simulated monthly totals for these stations is mostly greater then 0.95. However, also, the precipitation cycle that appears to be not so pronounced (Kozani) is with the exception of October and December satisfactorily reproduced.

The precipitation diagnostics was done for three stations with different elevations ranging from 4 m asl for Corfu to 627 m asl for Kozani (Table 10). Whereas, Agrinio and Corfu have typical seasonal precipitation cycle, the average monthly precipitation amounts for Kozani are approximately the same during the year. The results show good agreement between observed and simulated precipitation series for all three stations. Like in the case of German stations the mean wet day amounts are slightly overestimated; however, only by 5–12%. The unconditional (π_W) and both conditional (P_{00} and P_{11}) probabilities are in very good agreement. Also other statistical tests like mean wet and dry spell length, number of dry spells with more then ten days in vegetation period and standard deviation of monthly precipitation totals showed that the model is able to reproduce all features of daily precipitation series under Greek climate conditions very well.

Examples of annual cycles of precipitation, its probability of occurrence and their Fourier approximations are presented in Figs. 14 and 15. Results of normalized spectral density analyses are again shown in Table 6. Because of the highly pronounced cycle of precipitation probability, the first harmonic explains almost all the variability of the annual cycle.

Annual cycle of autocorrelation for observed series is quite well pronounced as presented in Fig. 16. From this figure, it follows that the persistence in the precipitation is higher in winter than in summer. The autocorrelation of the simulated precipitation series is in good accordance with this for observed series. The spatial covariance is very important for areal precipitation. However, in the Greek example the stations are so far apart that a meaningful covariance could not be identified.

4. Discussion and conclusions

In this paper a model for generating daily precipitation series and two case studies have been presented. Because the precipitation characteristics depend on large-scale atmospheric circulation conditions, the conditional precipitation characteristics for each circulation pattern are computed. It is generally possible to take arbitrary number of precipitation stations into account and therefore the process can be described as multivariate stochastic one. The seasonal cycle of precipitation is simulated by using Fourier series. The statistical comparison of observed and simulated precipitation series performed according to Wilby et al. (1998b) showed that most features are in very good agreement. The relatively poor inter-annual performance of the model (Figs. 4 and 12) is caused by the aggregation in time and by the statistical character of CP conditioning. May be additional variables could improve quality of the inter-annual performance (measures of vertical stability, humidity etc.) However, it is necessary to strenghten, that the model was developed with the main aim to generate daily precipitation series, which would have properties of the observed ones. The successful result of this objective is demonstrated in the diagnostics tables (Tables 5 and 10). The generated precipitation time series can be used as input data in various types of hydrological models. Especially for determining of design floods these models require long precipitation series, which are very often not available.

The results of this paper can be summarized as follows:

1. A model for downscaling daily precipitation has been developed. The rainfall is modeled as process coupled to atmospheric circulation — it is linked to the circulation patterns using conditional probabilities.
2. The annual cycle of model parameters including autocorrelation and spatial correlation is taken

into account and modeled by means of Fourier series.

3. The model can use any kind of classification of circulation patterns. In this study an objective automated fuzzy rule based classification of circulation patterns was applied, which needs atmospheric pressure data in regular grid as input.
4. The model was successfully applied in two regions with different climate conditions: Central Europe (Germany) and Eastern Mediterranean (Greece).
5. Several tests like comparison of monthly precipitation averaged over the validation period, comparison of mean values and deviations of yearly totals and other standard diagnostics showed that simulated values agree fairly well with historical data.
6. The model enables generating of long precipitation series which can be used as input to hydrological modeling focused on extremes with long recurrence intervals (like floods, severe droughts). In addition to this, precipitation observations in a catchment are often from different length, which means that hydrological simulations are based on precipitations obtained from different observation station configurations. However, long series of precipitation can be generated for a great number of stations based on much shorter common observations.

References

Bárdossy, A., Plate, E.J., 1991. Modeling daily rainfall using a semi-Markov representation of circulation pattern occurence. J. Hydrol. 122, 33–47.

Bárdossy, A., Plate, E.J., 1992. Space-time model of daily rainfall using atmospheric circulation patterns. Water Resour. Res. 28 (5), 1247–1259.

Bárdossy, A., Stehlík, J., Caspary, H.-J., 2001. Automated optimized fuzzy rule based circulation pattern classification for precipitation and temperature downscaling. Submitted for Publication.

Baur, F., Hess, P., Nagel, H., 1944. Kalendar der Grosswetterlagen Europas 1881–1939. Bad Homburg.

Berger, A., Goossens, C., 1983. Persistence of dry and wet spells at Ucle (Belgium). J. Climatol. 3, 21–34.

Binark, A.-M., 1979. Simultane Niederschlagsgenerierung an mehreren Stationen eines Einzugsgebietes, IHW Mitteilungen, Heft 16, Karlsruhe.

Blažková, Š., Beven, K., 1997. Flood frequency prediction for data limited catchments in the Czech Republic using a stochastic rainfall model and TOPMODEL. J. Hydrol. 195 (1–4), 256–278.

Bras, R.-S., Rodriguez-Iturbe, I., 1985. Random Functions in Hydrology. Addison-Wesley, Reading, MA 559pp.

Bürger, K., 1958. Zur Klimatologie der Großwetterlagen, Ber. Dtsch. Wetterdienstes 45, vol. 6, Selbstverlag des Deutschen Wetterdienstes, Offenbach am Main, Germany.

Chang, T.-J., Kavvas, M.-L., Delleur, J.-W., 1984. Modeling of sequences of wet and dry days by binary discrete autoregressive moving average processes. J. Climate Appl. Meteorol. 23, 1367–1378.

Colman, A., Davey, M., 1999. Prediction of summer temperature, rainfall and pressure in Europe from preceding winter North Atlantic ocean temperature. Int. J. Climatol. 19, 513–536.

Foufoula-Georgiou, E., Lettenmaier, D.-P., 1987. A Markov renewal model for rainfall occurences. Water Resour. Res. 23, 875–884.

Giorgi, F., Mearns, L.-O., 1991. Approaches to the simulation of regional climate change — a review. Rev. Geophys. 29, 191–216.

Hay, L.-E., McCabe, G.-J., Wolock, D.-M., Ayers, M.-A., 1991. Simulation of precipitation by weather type analysis. Water Resour. Res. 27, 493–501.

Hay, L.-E., McCabe, G.-J., Wolock, D.-M., Ayers, M.-A., 1992. Use of weather types to disaggregate general circulation model predictions. J. Geophys. Res. 97, 2781–2790.

Henze, N., Klar, B., 1993. Goodness-of-Fit Testing for a Space-Time Model for Daily Rainfall. Institut für Wissenschaftliches Rechnen und Mathematische Modellbildung, Universität Karlsruhe, Preprint No. 93/6, 21pp.

Hess, P., Brezowsky, H., 1969. Katalog der Großwetterlagen Europas. 2. Neu bearbaitete und ergänzte Aufl. Berichte des Deutschen Wetterdienstes 113, Selbstverlag des DWD, Offenbach a. Main.

Huth, R., 1997. Potential of continental-scale circulation for the determination of local daily surface variables. Theor. Appl. Climatol. 56, 165–186.

Huth, R., Kyselý, J., 2000. Constructing site-specific climate change scenarios on a monthly scale using statistical downscaling. Theor. Appl. Climatol. 66, 13–27.

IPCC, 1996. Climate change 1995. Impacts, Adaptations and Mitigation of Climate Change: Scientific-Technical Analyses, Cambridge University Press, Cambridge Contribution of Working Group I to the Second Assessment Report of the Intergovernmental Panel on Climate Change.

Jayawardena, A.-W., Lai, F., 1994. Analysis and prediction of chaos in rainfall and stream flow time series. J. Hydrol. 153, 28–52.

Karl, T.-R., Wang, W.-C., Schlesinger, M.-E., Knight, R.-W., Portman, D., 1990. A method of relating general circulation model simulated climate to the observed local climate Part I: seasonal statistics. J. Climate 3, 1053–1079.

Katz, R.-W., Parlange, M.-B., 1993. Effects of an index of atmospheric circulation on stochastic properties of precipitation. Water Resour. Res. 29, 2335–2344.

Katz, R.-W., Parlange, M.-B., 1996. Mixtures of stochastic processes: application to statistical downscaling. Climate Res. 7, 185–193.

Koutsoyiannis, D., 1999. Optimal decomposition of covariance matrices for multivariate stochastic model in hydrology. Water Resour. Res. 35 (4), 1219–1229.

Koutsoyiannis, D., Xanthopoulos, Th., 1990. A dynamic model for short-scale rainfall disaggregation. Hydrol. Sci. J. 35 (3), 303–322.

Laevesley, G.-H., 1994. Modeling the effects of climate change on water resources — a review. Climat. Change 28, 159–177.

Lamb, H.-H., 1972. British Isles weather types and a register of daily sequence of circulation patterns 1861–1971. Geophys. Mem. No. 110, 85 Meteor. Office, London.

Lamb, H.-H., 1977. Climate, Present, Past and Future. , Climatic History and the Future, vol. 2. Methuen and Co Ltd, London 835pp.

Lorenz, E.-N., 1969. The predictability of a flow which possesses many scales of motion. Tellus 21, 289–307.

Maheras, P., 1988. The synoptic weather types and objective delimitation of the winter period in Greece. Weather 43, 40–45.

Maheras, P., 1989. Delimitation of the Summer-dry period in Greece according to the frequency of weather-types. Theor. Appl. Climatol. 39, 171–176.

Mamassis, N., Koutsoyiannis, D., 1993. Structure Stochastique des Pluies Intenses Par Type de Temps, vol. 6. Publications de l'Association Internationale de Climatologie, Thesssaloniki pp. 301–313.

Mamassis, N., Koutsoyiannis, D., 1996. Influence of atmospheric circulation types in space-time distribution of intense rainfall. J. Geophys. Res.-Atmos. 101 (D21), 26267–26276.

Rodriguez-Iturbe, I., Cox, D.-R., Isham, V., 1987. Some models of rainfall based on stochastic point processes. Proc. R. Soc. London, A 410, 269–288.

Rodriguez-Iturbe, I., Febres de Power, B., Sharifi, M.-B., Georgakakos, K.-P., 1989. Chaos in rainfall. Water Resour. Res. 25 (7), 1667–1675.

Sharifi, M.-B., Georgakakos, K.-P., Rodriguez-Iturbe, I., 1990. Evidence of deterministic chaos in the pulse of storm rainfall. J. Atmos. Sci. 47 (7), 888–893.

Sivakumar, B., 2000. Chaos theory in hydrology: important issues and interpretations. J. Hydrol. 227 (1–4), 1–20.

Sivakumar, B., Liong, S.-Y., Liaw, C.-Y., 1998. Evidence of chaotic behaviour in Singapore rainfall. J. Am. Water Resour. Assoc. 34 (2), 301–310.

von Storch, H., Zorita, E., Cubasch, U., 1993. Downscaling of global climate change estimates to regional scales: an application to Iberian rainfall in wintertime. J. Climate 6, 1161–1171.

Trenberth, K.-E., 1990. Recent observed interdecadal climate changes in the Northern hemisphere. Bull. Am. Meteorol. Soc. 71, 988–993.

Wigley, T.-M.-L., Jones, P.-D., Briffa, K.-R., Smith, G., 1990. Obtaining sub-grid scale information from coarse resolution general circulation model output. J. Geophys. Res. 95, 1943–1953.

Wilby, R.-L., Wigley, T.-M.-L., 1997. Downscaling general circulation model output: a review of methods and limitations. Progress Phys. Geogr. 21, 530–548.

Wilby, R.-L., Hassan, H., Hanaki, K., 1998a. Statistical downscaling of hydrometeorological variables using general circulation model output. J. Hydrol. 205, 1–19.

Wilby, R.-L., Wigley, M.-L., Conway, D., Jones, P.-D., Hewitson, B.-C., Main, J., Wilks, D.-S., 1998b. Statistical downscaling of general circulation model output: a comparison of methods. Water Resour. Res. 34 (11), 2995–3008.

Wilby, R.-L., Hay, L.-E., Leavesley, G.-H., 1999. A comparison of downscaled and raw GCM output: implications for climate change scenarios in the San Juan River basin, Colorado. J. Hydrol. 225, 67–91.

Wilks, D.-S., 1989. Conditioning stochastic daily precipitation models on total monthly precipitation. Water Resour. Res. 25, 1429–1439.

Wilson, L.-L., Lettenmaier, D.-P., Wood, E.-F., 1991. Simulation of precipitation in the Pacific Northwest using a weather classification scheme. Survey Geophys. 12, 127–142.

Wilson, L.-L., Lettenmaier, D.-P., Skyllingstad, E., 1992. A hierarchical stochastic model of large-scale atmospheric circulation patterns and multiple station daily rainfall. J. Geophys. Res. 97 (ND3), 2791–2809.